

Dual role of copper on the reactivity of activated carbons from coal and lignocellulosic precursors

Haro M^a, Ruiz B^a, Andrade M^b, Mestre AS^b, Parra JB^a, Carvalho AP^{b*}, Ania CO^{*a}

^a Instituto Nacional del Carbón, INCAR-CSIC, Apdo. 73, 33080 Oviedo, Spain

^b Departamento de Química e Bioquímica and CQB, Faculdade de Ciências da Universidade de Lisboa, Ed. C8, Campo Grande, 1740-16 Lisboa, Portugal

*Corresponding author. Tel: + 351 217500897 / + 34 985 118846
E-mail address: apcarvalho@fc.ul.pt (AP Carvalho); conchi.ania@incar.csic.es (CO Ania)

Abstract

The synthesis of copper-doped activated carbons from different origin (i.e., lignocellulosic and bituminous coal) by a wet impregnation and low temperature calcination procedure has been explored, as well as the role of copper particles on the physicochemical and structural features of the resulting materials. The textural characterization and isothermal reactivity analysis of the pristine and doped activated carbons have shown that the role of copper during the calcination step strongly depended on the nature of the carbon matrix. Copper impregnation of a coal-derived activated carbon catalyzed the air gasification of the material at a very low temperature (i.e., 325 °C), bringing about the development of microporosity on the doped carbon. In contrast, when copper was immobilized on a lignocellulose-derived activated carbon, the metallic species act as combustion retardant during the calcination step, protecting the carbon matrix during the catalytic gasification. In

both cases, the resulting materials displayed a homogenous distribution of copper within the carbon matrix, while preserving large textural properties.

Keywords: activated carbon; copper; isothermal gasification

1. Introduction

Activated carbons are extensively used in a large number of industrial applications, mainly covering adsorption (both in gas and aqueous phase) and catalytic processes [1-3]. This is due to their low cost, wide availability and high performance, owing to their flexible coordination chemistry that allows an infinite possibility of three-dimensional structures with expanded pore network, and to their ability to react with other heteroatoms on the surface or within the structural framework.

In many applications, knowledge of the surface chemistry of carbons is of paramount importance as it determines the chemical stability and the reactivity in adsorptive and catalytic processes [4, 5]. A high number of activated carbon applications have arisen because of the existence of a superficial layer of chemically bonded elements. Very often, the natural chemistry of an activated carbon surface (usually coming from the precursor or activation agent) is not potent enough to promote specific adsorbate-adsorbent interactions or catalytic properties of the carbon surfaces. Thus, the possibility of enhancing the physicochemical properties of carbons via modification of their surface by the incorporation of the desired heteroatoms is among current research interests in carbon science.

In this regard, various methods have been described in the literature to modify carbon surface chemistry [6-9]. Particularly, the incorporation of transition metals of

catalytic activity on porous solids (including zeolites, pillared clays and carbonaceous materials) has attracted widespread interest for some decades due to the potential applications of such materials in catalytic and adsorption processes [1, 3, 10, 11]. This is the result of the demand for highly functionalized materials in emergent areas, where besides tailoring the porosity (efforts are concentrated in the synthesis of carbons with tailorable pore sizes, controlled pore shapes and large surface areas), the surface chemistry of the obtained materials plays a crucial role to develop selective adsorbents and more efficient catalysts.

To meet such demands many approaches have been explored; the incorporation of the metal has been made in the precursor of the activated carbon, directly in the activated carbon, by means of oxidation treatments, impregnation with metal oxides or metal chlorides, carbonization of polymers of organic salts with metals on its composition, and so forth [12-18]. In all cases it is crucial to obtain a high dispersion and distribution of the metal in the carbon, while developing or maintaining the porosity of the support.

The objective of this work was to explore the dual role of copper as activating and protective agent of activated carbons of different nature (i.e., lignocellulosic and coal precursors). The presence of the metal in the carbon materials may enhance their catalytic [19], redox [20, 21], or adsorptive properties [14, 22, 23]. We have focused on the study of the porous structure and the metal content and dispersion of doped carbon materials. In a typical procedure, the carbon material was impregnated with the inorganic salt containing the selected metal (i.e., copper nitrate) and calcined. The effect of the carbon precursor on the dispersion of the metallic species and the porosity of the resulting metal doped carbons has been investigated; these features of paramount interest to prepare

copper-doped carbons with a homogenous distribution of the metallic species on the carbon matrix and large surface areas.

2. Experimental Methods

2.1 Materials

Two activated carbons obtained from different precursors were selected: a lignocellulosic-derived activated carbon obtained from CO₂ activation (800 °C, 1 h) of sisal (*Agave Sisalana*) fibers (S), and a commercially available activated carbon obtained from steam activation of a bituminous coal precursor (Q). Copper nitrate (Sigma Aldrich, 99 % purity) was used as inorganic salt precursor. The metal loaded carbons were prepared by a wet impregnation technique using an aqueous solution of the copper salt. About 20 mL of this solution were put in contact with 1 g. of activated carbon and stirring for 24 hours. The solution concentration was adjusted to attain 1 wt.% copper in the activated carbons. Impregnated samples were dried overnight at 100 °C in an air recirculation oven and then calcined at 325 °C for 3 h in air atmosphere (2 °C/min). The calcination step allowed the removal of the counter-ion of the metallic cation and thus to fix the metallic species on the carbon matrix. The calcined copper-loaded samples will be referred to as SCu and QCu. Blanks of the raw non-impregnated activated carbons calcined at the same temperature were also prepared (labeled as Scal and Qcal).

2.2 Characterization of the carbon materials

Textural characterization of the carbon materials was carried out by N₂ and CO₂ adsorption-desorption isotherms at -196 and 0 °C, respectively. Before the experiments,

the samples were outgassed under secondary vacuum at 120 °C overnight. The isotherms were used to calculate the specific surface area, S_{BET} , total pore volume, V_{T} (evaluated at p/p° 0.95), and pore size distributions using the density functional theory (DFT) approach [24]. The volume of narrow micropores was evaluated from the DR formulism applied to the CO_2 adsorption data, using 1.023 g/cm^3 as the density of adsorbed CO_2 and 0.36 as the value of the β parameter. Elemental analysis of the raw carbons was carried out in LECO automatic analyzers (LECO CHNS-932 and LECO VTF-900 for the oxygen content).

The samples were further characterized by thermogravimetric analysis (Setaram Labsys) employing the following instrument settings: heating rate of $15 \text{ }^{\circ}\text{C min}^{-1}$; nitrogen and air atmosphere at a flow rate of 50 mL min^{-1} . X-ray diffraction (XRD) patterns were recorded on a Bruker D8 Advance instrument operating at 40 kV and 40 mA, and using $\text{Cu K}\alpha$ ($\lambda = 0.15406 \text{ nm}$) radiation. Dispersion of the metallic particles incorporated to the carbon matrices was characterized using a Ziess DSM 942 scanning electron microscope; particles were dispersed on a graphite adhesive tab placed on an aluminum stub. The images were generated in the back scattered electron signal mode, which yielded better quality pictures.

Reactivity measurements of the impregnated carbons before calcination were carried out in dry air at 325 °C in a thermobalance. The sample (ca. 10-15 mg) was initially heated under N_2 up to 325 °C (50 mL min^{-1}), and then the nitrogen flow was changed to dry air and maintained during 3 hours. The flow was changed again to nitrogen during the cooling down experiments. The reactivity tendency in air was corrected versus the corresponding blank experiments in inert atmosphere.

3. Results and discussion

3. 1. Characterization and reactivity of the raw activated carbons

Nitrogen adsorption isotherms presented in Figure 1 illustrate the evolution of porosity from the pristine (samples S and Q) to the copper-loaded final activated carbons (samples SCu and QCu). Additionally, the corresponding textural parameters evaluated are presented in Table 1. As it can be observed in Figure 1, the pristine carbons before copper impregnation exhibit a hybrid I/IV isotherm according to the IUPAC classification, which is characteristic of microporous materials with an important contribution of mesoporosity [25]. Both raw activated carbons show a broad knee at relative pressures $p/p^0 \sim 0.2$, suggesting the presence of wide micropores. The N_2 adsorption isotherms also show a hysteresis loop (type H4) at relative pressures about 0.5 where the adsorption and desorption branches are parallel, that indicates the presence of small slit-shaped pores and a well developed mesoporosity for both carbons [25]. An exhaustive analysis of the distribution of pore sizes was carried out combining the information of N_2 and CO_2 adsorption isotherms (Figure 2). In the case of sample Q, the micropore volume obtained by the DR equation applied to N_2 was larger than that obtained from CO_2 adsorption, indicating the presence of wide micropores (disregarding kinetic restrictions) [26]. The opposite trend was obtained for sample S, showing the contribution of the narrow micropores for this material.

It can be observed that the calcination at 325 °C brought about quite a different response of both activated carbons, with important modifications in the textural properties for the sisal-derived sample. In the case of the coal-derived activated carbon (Qcal), a slight increase in the oxygen content was observed (Table 2) after calcination,

which indicates that oxidation of the carbonaceous matrix was the dominant reaction taking place during the calcination of this activated carbon [27]. This behavior was somewhat expected based on the low temperature chosen for the calcination treatment, which aimed at decomposing the counter-anion of the copper salts while preventing the gasification reaction under air atmosphere (which did not seem to occur at 325 °C). Indeed, both the thermal analysis of the inorganic salt used in the impregnation and the DTG profiles of the raw carbon Q in air (Figure 3 and inset) confirmed both observations: the complete decomposition of copper nitrate below 325 °C and the inertness of carbon Q at these conditions. Consequently, minor changes in the textural properties of carbon Q were detected upon calcination (sample Qcal). The slight decrease in the surface area and pore volumes (accounting for ca. 10 %), can be attributed to the slight oxidation of the matrix (Table 2). Although some works in the literature report that air gasification of carbon materials at moderate temperatures (between 300-500 °C) leads to an increase in the mesopore volume of activated carbons [28], our results show that this was not the case of sample Q, at least for the non catalytic gasification. The study of the reactivity of carbon Q in air in a thermobalance (isothermal gasification) also confirmed that this carbon does not react with air under these conditions, even when long times (ca. 3 hours) are applied (Figure 4).

In contrast, calcination brought about a severe modification of the sisal derived activated carbon. This sample (Scal) was almost completely burnt-out when exposed to air at 325 °C during 3 hours (mass loss 23 %), and the resulting material had a negligible porosity (Figures 1 and 2) and a grayish color (see inset in Figure 2). This structural collapse suggests that a strong gasification of this lignocellulose-derived activated carbon

takes place at 325 °C, as opposed to what was observed for carbon Q. In fact, the fast calcination of the sisal-derived activated carbon was confirmed by the reactivity studies in the thermobalance). It can be observed in Figure 3 that mass loss of the lignocellulose-derived activated carbon in air becomes to be important at temperatures above 280 °C, below the temperature chosen for the calcination treatment in this study. Moreover, the isothermal gasification tests at 325 °C (Figure 4) confirmed an overall mass loss close to 25 wt.% after 3 hours, as opposed to 0.5 wt.% for the coal-derived carbon.

Although the non-catalytic gasification of biomass-derived chars at low temperatures has been reported in the literature [29], an important difference here is that in our study the air gasification has been carried out in an activated carbon (not on the solid residue after pyrolysis of the biomass, this is a 'char'). Sample S, being an activated carbon, has already been exposed to high temperatures during the activation step and consequently the amount of volatiles resulting from the thermal cracking of the carbon matrix is not very high (ca. below 7 wt.%, and similar to that of carbon Q). Thus, the high reactivity towards air exposure of this carbon can be associated to the presence of highly reactive sites in this material, likely as a result of the rich surface chemistry (Table 2) characteristic of lignocellulose-derived carbons.

3. 2. Characterization and reactivity of the copper-doped activated carbons

When copper was incorporated to the carbon matrix, outstanding differences were obtained for both materials, particularly if one bears in mind the low amount of metal (ca. 1 %) immobilized. It can be observed from the gas adsorption isotherms that the impregnation of copper brought about an important porosity development (Figures 1 and 2) in both cases. This effect was undoubtedly more pronounced for the lignocellulose-

derived activated carbon, where copper impregnation appeared not only to promote the air gasification but to prevent the complete calcination and further structural collapse of the pristine activated carbon. Since this effect was not observed for the corresponding non-impregnated calcined carbons, it has to be attributed to the copper incorporated to the carbon matrix.

In the case of sample Q, the catalytic effect of copper for the air gasification was evident on the textural parameters of the resulting carbon (Table 1). It was also corroborated by the reactivity studies in the thermobalance. The DTG profiles under air (Figure 3) of the impregnated copper-carbon (sample QCu before calcination) showed that the onset of the calcination reaction of the copper-doped carbon Q occurred at about 200 °C lower than that of the pristine activated carbon Q. The isothermal gasification at 325 °C during 3 hours also confirmed the higher mass loss (ca. 7 wt.%) of the copper impregnated activated carbon (Figure 4).

The catalytic activity of copper as well as other transition metals on the gasification of carbons is rather well known, due to their ability to undergo oxidation-reduction reactions at the carbon-metal interface [30-33]. However, most studies have reported this behavior in chars obtained from various precursors and at higher temperatures than those herein used. This is an important advantage, since reducing the activation temperature might limit the sintering of copper particles, thus enabling a better distribution of the metallic species on the resulting carbon material.

Moreover, we have observed that the gasification causes mainly an enlargement of the microporous structure of Q carbon (N_2 adsorption isotherms are parallel from relative pressures above 0.3). Analysis of the gas adsorption data revealed that the narrow

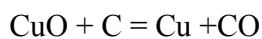
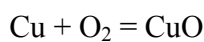
microporosity -determined by the CO₂ adsorption isotherms- of the pristine carbon remained rather unchanged, and that the modifications in the pore volume and surface area are associated to an enlargement of the micropores of wider sizes. It is also interesting to remark that the incorporation of copper to activated carbons has been reported to provoke a collapse in the porosity of the metal-loaded carbons [34, 35].

In the case of the lignocellulose-derived activated carbon (sample SCu), the effect of copper is more striking, as it seems to provoke the opposite effect. Calcination of the non-impregnated sample (Scal) at 325 °C was very strong, which caused a remarkable damage in the carbon structure and porosity. In contrast, the mass loss after 3 hours of calcination decreased from 23 to 7 wt.% when copper was incorporated to this material (Figure 4). Indeed, the DTG profiles in air show that the onset temperature of the calcination is delayed ca. 60 °C, compared to the pristine sisal-derived activated carbon (Figure 3). As results of this, a slight pore development in the copper-doped material was obtained, rather than its burning-out (Table 1). Thus, although it is evident that the gasification reaction occurs (similarly to carbon Q), it would seem that copper plays another role here, behaving as gasification retardant as opposed to what has been reported so far for the role of copper in the gasification of coal and lignocellulosic chars [30, 36, 37].

The SEM images and XRD analysis of the copper-loaded carbon materials (QCu and SCu) were used to further investigate the distribution of the copper species on the surface of the doped carbons. The SEM micrographs (Figure 5) show no visual signs of the impregnation (no arrays of copper clustering); according to EDX analysis, the white particles observed in the micrographs correspond to the mineral matter of the carbons.

Moreover, the EDX screening of bigger areas (see red mark in Figure 5) of the carbon particles (in both cases) show copper distributed within the carbon matrix. This confirms that copper is homogeneously distributed on the carbon, rather than forming large copper clusters. The low amount of copper incorporated to the carbon matrix (ca. 1 wt.%) compared to other studies might be responsible for the even distribution of the copper species, preventing the formation of large particle aggregates [14]. XRD of these samples confirmed the co-existence of copper oxides and metallic Cu on the carbon matrix. These results also indicate the good dispersion of the metallic salt before calcination, and thus a relatively strong Cu-carbon interaction in both activated carbons. The elemental analysis data of the studied carbons indicated that along with copper, quantities of oxygen were also incorporated to the carbon matrix during the calcination treatment (Table 2). The SEM image of SCu also shows that the calcination did not destroy the fibrous structure of the sisal-derived material, as it was the case for calcination in the absence of copper.

The catalytic gasification of copper on carbons (graphites and chars) has been explained by the mobility of confined Cu/CuO nanoparticles [37-39] at temperatures close to the Tamman value (i.e. temperature at which sintering starts). This mobility is valid for particles below a critical size (below 100 nm), and facilitates the diffusion of oxygen to the copper-carbon interface when the material is exposed to air, thereby favoring oxidation-reduction reactions according to:



The SEM images (Figure 5) confirmed the small size of the copper particles in both materials, for which migration of the metallic species is not restricted. However,

325 °C is far below the Tamman temperature reported for Cu and CuO (405 and 527 °C, respectively [36]), although mobility of copper particles could still be possible by an extra heat arisen from other redox reactions occurring at the carbon surface [36]. This could be the case for the gasification of sample Q, in which the extra-heat may come from the thermal decomposition of the nitrate ion (inset in Figure 3).

In the case of sisal-derived activated carbon, the situation seems more complex. As mentioned above, the rich surface chemistry (Table 2) of this activated carbon could explain the easier gasification in air and in the absence of a metallic catalyst. The impregnation with copper somehow protects this material from the fast oxidation, as if the copper species would create an inert film on the carbon surface that would prevent the reactions when this is exposed to air. A somewhat similar role of copper salts as flame retardants of thermoplastic polymers has been reported in the literature [40]. However its effect on the delay of the combustion of an activated carbon (protection) had not been previously reported. Moreover, the good dispersion of the copper particles within the carbon matrix (no large aggregates are observed) along with the preservation of the porous structure and the increased oxidation resistance make these copper-loaded carbons excellent candidates to be used as catalysts in advanced oxidation processes for the degradation of refractory pollutants.

4. Conclusions

This work describes the dual role of copper as both catalyst and chemical protector (i.e., combustion retardant) during the calcination of activated carbon materials from different origins (i.e., lignocellulose and coal-derived). In the case of a coal-derived

activated carbon, the immobilization of copper on the carbon matrix catalyzes the air gasification, by lowering the calcination temperature by 100 °C. As a result of the low temperature, the sintering of metallic species is avoided and the resulting material presented a homogenous dispersion of metallic particles within the carbon matrix, while displaying an enlargement of the existing microporous network (to mesopores). On the other hand, the copper immobilized on a highly reactive lignocellulosic activated carbon prevented the structural collapse of the materials during calcination, while promoting the porosity development. In this case, a dual role of copper particles was observed, acting as a protective layer of the carbon (to avoid its burning out), and enlarging the microporosity to create mesopores. These materials showing a good dispersion of nanosized copper particles and large textural development are promising candidates as highly selective adsorbents and catalysts to be used in advanced remediation techniques.

Acknowledgments

The authors thank the Spanish MICINN for financial support (projects CTM2008-01956/TECNO and Acción Integrada AIB2010PT-00209). MH thanks CSIC for a postdoctoral contract. MA thanks FCT for her PhD fellowship (SFRH/BD/71673/2010). The authors also thank Cordex for kindly providing the sisal residues.

REFERENCES

- [1] J.L. Figueriedo, Carbon Materials for Catalysis, Serp Ph, John Wiley and Sons, New Jersey, 2009.
- [2] H. Marsh, F. Rodriguez-Reinoso, Activated Carbon, Elsevier, Oxford, 2006.
- [3] D. Nguyen-Tahn, T.J. Bandoz, Microporous Mesoporous Mat. 92 (2006) 47-55.
- [4] C.O. Ania, T.J. Bandoz, Energy Fuels. 20 (2006) 1076-1080.

- [5] L.R. Radovic, C. Moreno-Castilla, J. Rivera-Utrilla, in: L.R. Radovic, L. R. (Ed.) *Chemistry and Physics of Carbon*, Marcel Dekker Inc., New York, 2001.
- [6] H. Oka, M. Inagaki, Y. Kaburagi, Y. Hishiyama, *Solid State Ion.* 121 (1999) 157-163.
- [7] F. Goutfer-Wurmser, H. Konno, Y. Kaburagi, K. Oshida, M. Inagaki, *Synth. Met.* 118 (2001) 33-38.
- [8] M. Inagaki, Y. Okada, H. Miura, H. Konno, *Carbon.* 37 (1999) 329-334.
- [9] C.W. Zhou, J. Kong, E. Yenilmez, H.J. Dai, *Science.* 290 (2000) 1552-1555.
- [10] R. Szosta, *Molecular Sieves Principles of Synthesis and Identification*, Van Nostrand Reinhold, New York, 1983.
- [11] C.O. Ania, T.J. Bandosz, *Microporous Mesoporous Mat.* 89 (2005) 315-324.
- [12] C. Petit, C. Karwacki, G. Peterson, T.J. Bandosz, *J. Phys. Chem. C.* 111 (2007) 12705-12714.
- [13] D. Hines, A. Bagreev, T.J. Bandosz, *Langmuir.* 20 (2004) 3388-3397.
- [14] C.O. Ania, T.J. Bandosz, *Carbon.* 44 (2006) 2404-2412.
- [15] C.O. Ania, T.J. Bandosz, *Stud. Surf. Sci. Catal.* 160 (2006) 559-566.
- [16] S. Hermans, A. Deffernez, M. Devillers, *Catalysis Today.* 157 (2010) 77-82.
- [17] M.A. Alvarez-Montero, L.M. Gomez-Sainero, A. Mayoral, I. Diaz, R.T. Baker, J.J. Rodriguez, *J. Catal.* 279 (2011) 389-396.
- [18] B.A. Qiu, L.N. Han, J.C. Wang, L.P. Chang, W.R. Bao, *Energy Fuels.* 25 (2011) 591-595.
- [19] J.H. Choy, H. Jung, Y.S. Han, J.B. Yoon, Y.G. Shul, H.J. Kim, *Chem. Mat.* 14 (2002) 3823-3828.
- [20] A. Sayari, *Chem. Mat.* 8 (1996) 1840-1852.
- [21] Q.H. Meng, L. Ling, H.H. Song, *J. Appl. Electrochem.* 36 (2006) 63-67.
- [22] G.X. Yu, J. Sun, X.M. Hou, X.L. Zhou, C.L. Li, L.F. Chen, J.A. Wang, in: J.A. Wang, G.Z. Cao, J.M. Dominguez (Eds.), *Advances in New Catalytic Materials*, Trans Tech Publications Ltd, Stafa-Zurich, 2010, pp. 133-140.
- [23] Z.J. Mei, Z.M. Shen, Q.J. Zhao, W.H. Wang, Y.J. Zhang, *J. Hazard. Mater.* 152 (2008) 721-729.
- [24] F. Rouquerol, J. Rouquerol, K. Sing, *Adsorption by Powders and Porous Solids*, Academic Press, London, 1999.
- [25] K.S.W. Sing, D.H. Everett, R.A.W. Haul, L. Moscou, R.A. Pierotti, J. Rouquerol, T. Siemieniowska, *Pure Appl. Chem.* 57 (1985) 603-619.
- [26] J.M. Juarez-Galan, A. Silvestre-Albero, J. Silvestre-Albero, F. Rodriguez-Reinoso, *Microporous Mesoporous Mat.* 117 (2009) 519-521.
- [27] H. Ogawa, K. Saito, *Carbon.* 33 (1995) 783-788.
- [28] A.R. Sánchez, A.A. Elguézabal, L. de La Torre Saenz, *Carbon.* 39 (2001) 1367-1377.
- [29] J. Gañan, J.F. Gonzalez, C.M. Gonzalez-Garcia, A. Ramiro, E. Sabio, S. Roman, *Appl. Surf. Sci.* 252 (2006) 5988-5992.
- [30] C. Moreno-Castilla, J. Rivera-Utrilla, A. López-Peinado, I. Fernández-Morales, F.J. López-Garzón, *Fuel.* 64 (1985) 1220-1223.
- [31] C. Moreno-Castilla, A. López-Peinado, J. Rivera-Utrilla, I. Fernández-Morales, F.J. López-Garzón, *Fuel.* 66 (1987) 113-118.
- [32] H. Marsh, B. Rand, *Carbon.* 9 (1971) 63-72, IN67-IN10, 73-77.

- [33] J.S.J. Vandeventer, M.A. Reuter, *Thermochim. Acta.* 137 (1989) 383-386.
- [34] D.J. Kim, J.E. Yie, *J. Colloid Interface Sci.* 283 (2005) 311-315.
- [35] S.J. Park, B.J. Kim, *J. Colloid Interface Sci.* 292 (2005) 493-497.
- [36] T.G. Devi, M.P. Kannan, G.N. Richards, *Fuel.* 69 (1990) 1440-1447.
- [37] R.T.K. Baker, J.J. Chludzinski Jr, *Carbon.* 19 (1981) 75-82.
- [38] D.W. McKee, *Carbon.* 8 (1970) 131-136, IN133-IN138, 137-139.
- [39] D.W. McKee, *Carbon.* 8 (1970) 623-626, IN625-IN627, 627-635.
- [40] G. Fontaine, T. Turf, S. Bourbigot, *Fire and Polymers V*, Chapter 20, ACS Symposium Series, 2009.

Figures Captions

Figure 1. N₂ adsorption isotherms at -196 °C of the pristine and copper-loaded activated carbons.

Figure 2. CO₂ adsorption isotherms at 0 °C of the studied activated carbons. Inset: images of the sisal-derived materials.

Figure 3. DTG profiles in air of the as-received and copper-doped samples.

Figure 4. Reactivity profiles of the isothermal air gasification at 325 °C for 3 hours of the pristine and copper-loaded samples.

Figure 5. SEM micrographs of the copper-loaded activated carbons and EDX analysis (qualitative) of the marked patch showing the distribution of heteroatoms on the carbon surface.

Tables Captions

Table 1. Main textural parameters of the activated carbons obtained from gas adsorption data.

Table 2. Elemental analysis [wt.%, DAF basis] of the pristine, copper-loaded and calcined activated carbons.

Table 1. Main textural parameters of the activated carbons obtained from gas adsorption data.

	S_{BET} [m ² g ⁻¹]	V_{TOTAL}^a [cm ³ g ⁻¹]	V_{MICRO}^b [cm ³ g ⁻¹]	V_{MESO}^b [cm ³ g ⁻¹]	$W_0, \text{N}_2 \text{ (DR)}^c$ [cm ³ g ⁻¹]	$W_0, \text{CO}_2 \text{ (DR)}^c$ [cm ³ g ⁻¹]
Q	1030	0.51	0.32	0.09	0.31	0.21
Qcal	976	0.48	0.301	0.08	0.36	0.21
QCu	1140	0.57	0.34	0.12	0.42	0.20
S	525	0.27	0.16	0.08	0.20	0.25
Scal	16	0.02	--	--	--	0.02
SCu	760	0.39	0.23	0.10	0.29	0.27

^a evaluated at $p/p_0 \sim 0.95$

^b evaluated from DFT applied to N_2 adsorption data

^c evaluated from DR equation

Table 2. Elemental analysis [wt.%, DAF basis] of the pristine, copper-loaded and calcined activated carbons.

	C [wt.%]	H [wt.%]	N [wt.%]	O [wt.%]	S [wt.%]
Q	96.3	0.6	0.7	2.1	0.3
Qcal	95.7	0.6	0.4	3.1	0.3
QCu	92.3	0.7	0.4	6.4	0.2
S	94.3	0.3	0.4	5.0	n.d.
Scal	-	-	-	-	-
SCu	90.9	0.5	0.5	8.1	n.d.

Figure 1.

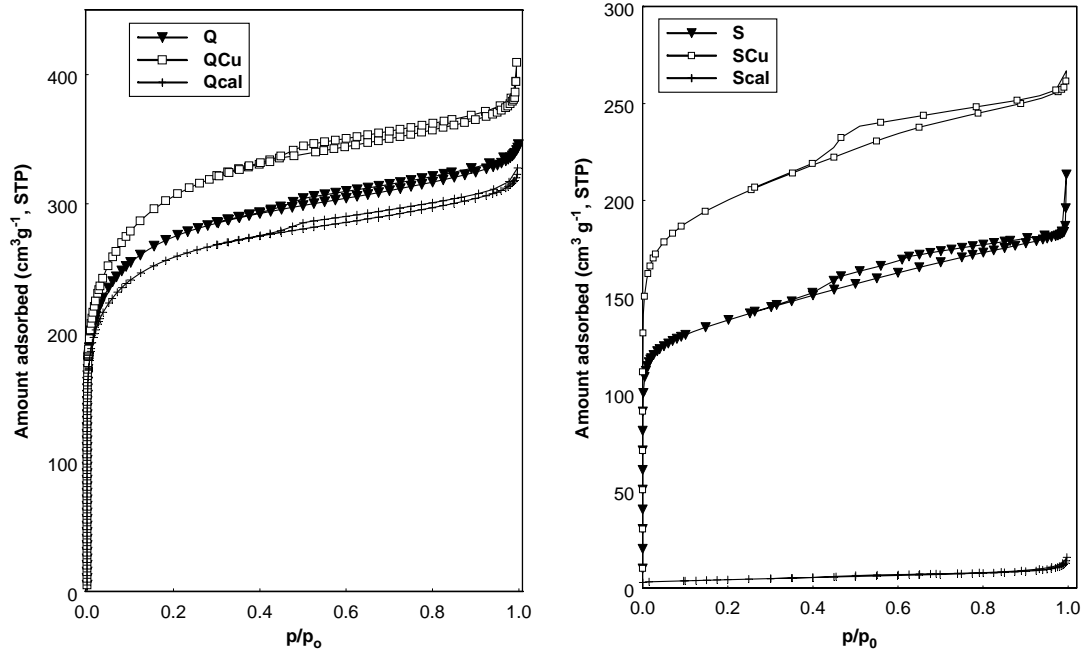


Figure 2.

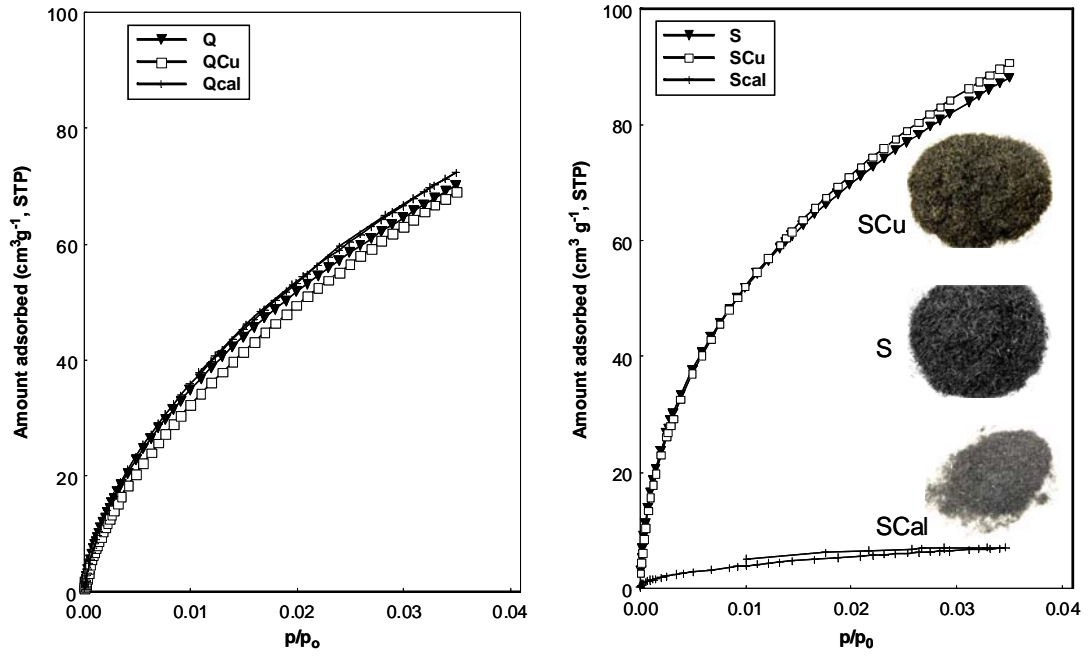


Figure 3.

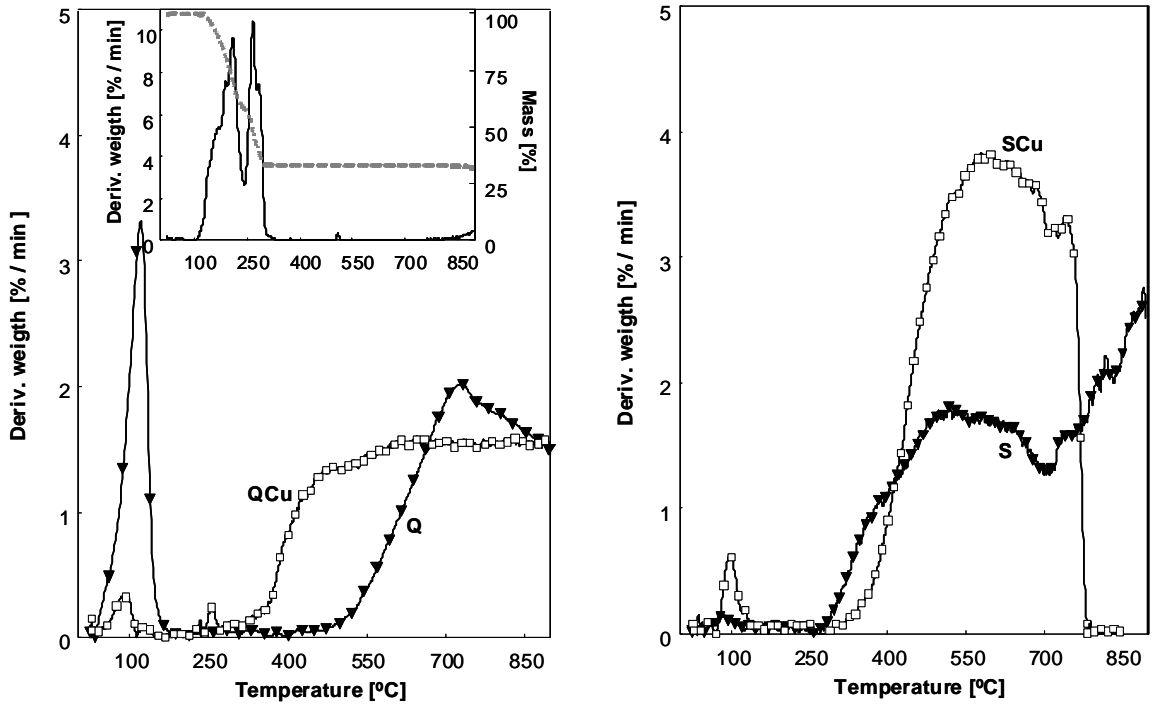


Figure 4.

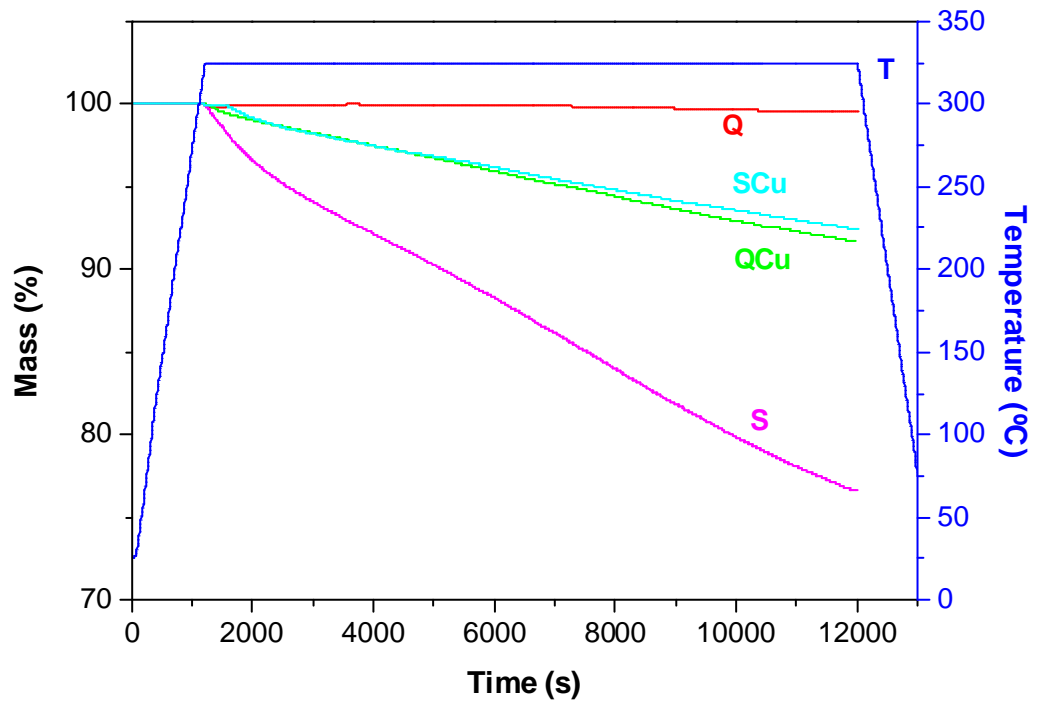


Figure 5.

